Structure of superheavy elements suggested in the reaction of ^{86}Kr with ^{208}Pb

J. Meng[1,2,3,*] and N. Takigawa[2]

[1]*Department of Technical Physics and Institute for Heavy Ion Physics, Peking University, Beijing 100871, People's Republic of China*

[2]*Department of Physics, Tohoku University, Sendai 980-8578, Japan*

[3]*Center of Theoretical Nuclear Physics, National Laboratory of Heavy Ion Accelerator, Lanzhou 730000, China*

(Received 10 August 1999; published 19 May 2000)

The structure of superheavy elements claimed to have been discovered in the recent ^{208}Pb(^{86}Kr,n) reaction at Berkeley is systematically studied in the relativistic mean field (RMF) approach. It is shown that various usually employed RMF forces, which give a fair description of normal stable nuclei, give different predictions for superheavy elements. Among the effective forces we tested, TM1 seems to be the best candidate to describe superheavy elements. The binding energies of the ^{293}118 nucleus and its α-decay daughter nuclei obtained using TM1 agree with those of FRDM within 2 MeV. A similar conclusion, that TM1 is the best interaction, is also drawn from the calculated binding energies for Pb isotopes with the relativistic continuum Hartree-Bogoliubov (RCHB) theory. Using the pairing gaps obtained from the RCHB and taking into account the blocking effect for neutrons, RMF calculations with deformation are carried out for the structure of superheavy elements. The binding energy, shape, single particle levels, and the Q values of the α-decay Q_α are discussed, and it is shown that the pairing correlation, blocking effect, and deformation are essential to properly understand the structure of superheavy elements. The Q_α values are calculated for the ground-state–to–ground-state transitions and for those respecting the angular momentum selection rule, and are compared with data.

PACS number(s): 21.60.Jz, 21.65.+f, 21.10.Gv, 27.90.+b

I. INTRODUCTION

Following the discovery of α-decay isotopes of elements $Z=110$, 111, and 112 at GSI [1–3], an isotope of element 118, ^{293}118, and several of its α-decay daughter nuclei were announced to have been discovered at Berkeley Lab's 88-Inch Cyclotron with the newly constructed Berkeley gas-filled separator by bombarding a lead target with an intense beam of krypton ions of 449 MeV [4]. The sequence of decay events is consistent with the long-standing theoretical prediction that there exists an ''island of stability'' around 114 protons and 184 neutrons and activates once again the study of superheavy elements.

The study of superheavy elements has been a hot topic for the last two decades. Recent works on the collisions, structure, and stability of heavy and superheavy elements can be found in Refs. [5–11]. In a recent paper, Smolanczuk claimed that the reaction ^{208}Pb(^{86}Kr,n) should have a particularly favorable production rate [12]. This motivated the experiment at Berkeley. According to the authors, the synthesized superheavy element ^{293}118 decays by emitting an α particle within less than a millisecond, leaving behind the isotope of element 116 with mass number 289. This daughter nucleus is also radioactive, α decaying to an isotope of element 114. The chain of successive α decays continues until element 106.

Smolanczuk discussed also the properties of superheavy elements in this mass region under the constraint of a spherical shape based on a macroscopic-microscopic approach [13]. In contrast to his approach, here we study the structure of the superheavy element ^{293}118 and of the daughter nuclei in the sequence of α decays in the relativistic mean field (RMF) theory. Microscopic study is essential to discussing α decay, because the macroscopic-microscopic approach allows us to discuss only the ground-state–to–ground-state decay, which is not obvious as we discuss later. The effects of deformation and pairing correlation as well as the blocking effect will be taken into account. The pairing gaps for deformed RMF calculations are taken from the spherical relativistic continuum Hartree-Bogoliubov (RCHB) theory [14], which is an extension of the relativistic mean field and the Bogoliubov transformation in the coordinate representation [15]. As the spin-orbit splitting which governs the shell structure and magic number is naturally obtained in the RMF theory, we expect that the structure of superheavy elements can be understood properly once the deformation, pairing correlation, and blocking effect are taken into account. We investigate the binding energy, deformation, the Q values of the α decay, the effect of pairing correlation, blocking effect, shell structure, and the structure of single-particle levels for protons and neutrons.

The paper is organized as follows. In Sec. II, we present the results of deformed RMF calculations without pairing correlation for several standard forces, which give a fair description of normal stable nuclei. We thus discuss the appropriate force to describe superheavy elements by comparing the results of ground-state properties with those suggested by the FRDM. In Sec. III the spherical RCHB theory is used to investigate the pairing correlation in these superheavy elements. The RCHB provides not only a unified description of mean-field and pairing correlation but also a proper description for the continuum and the coupling between the bound state and the continuum [14]. We then perform in Sec. IV the study by a deformed RMF+BCS approach using the pairing gaps supplied by RCHB for protons and neutrons. We summarize the paper in Sec. V.

*Electronic address: meng@ihipms.ihip.pku.edu.cn

TABLE I. The binding energy E of the superheavy element $^{293}118$ and of its α decay daughter nuclei calculated in the RMF theory with effective interactions TM1, NL1, NL3, and NLSH. The K quantum number and the parity of the last filled neutron orbit are also included. The prediction of FRDM is given in the last column.

Nucleus	TM1		NL1		NL3		NLSH		FRDM
$^{A}Z_{N}$	E (MeV)	Ω^{π}	E (MeV)	Ω^{π}	E (MeV)	Ω^{π}	E (MeV)	Ω^{π}	E (MeV)
$^{265}104_{161}$	1949.2	$7/2^{+}$	1953.0	$11/2^{-}$	1951.1	$3/2^{+}$	1950.5	$7/2^{+}$	1950.0
$^{269}106_{163}$	1970.2	$7/2^{+}$	1974.1	$5/2^{+}$	1970.5	$7/2^{+}$	1977.5	$7/2^{+}$	1970.5
$^{273}108_{165}$	1990.2	$13/2^{-}$	1992.8	$3/2^{+}$	1990.7	$13/2^{-}$	1997.9	$13/2^{-}$	1989.4
$^{277}110_{167}$	2007.9	$5/2^{+}$	2010.5	$13/2^{-}$	2009.0	$5/2^{+}$	2016.1	$5/2^{+}$	2007.0
$^{281}112_{169}$	2026.2	$3/2^{+}$	2029.8	$1/2^{+}$	2027.7	$3/2^{+}$	2034.7	$3/2^{+}$	2025.2
$^{285}114_{171}$	2041.3	$3/2^{-}$	2051.8	$1/2^{+}$	2045.1	$1/2^{+}$	2048.7	$5/2^{+}$	2044.1
$^{289}116_{173}$	2058.2	$5/2^{-}$	2068.7	$9/2^{+}$	2062.1	$9/2^{+}$	2065.6	$5/2^{+}$	2061.1
$^{293}118_{175}$	2074.7	$3/2^{+}$	2088.9	$3/2^{+}$	2079.8	$3/2^{+}$	2080.5	$3/2^{+}$	2077.2

II. EXAMINATION OF VARIOUS RMF PARAMETER SETS

There are many parameter sets for RMF calculations, which provide nearly equal quality of description for stable nuclei. Therefore, we wish to find at first which effective force in RMF is more suitable to describe superheavy elements. As claimed in Ref. [11] the results are strongly interaction dependent. For this purpose we perform RMF calculations that include deformation but ignore pairing correlations with different effective forces in the axially symmetric case. The details of the method can be found in Ref. [16]. The coupled Dirac equation for nucleons and the Klein-Gordon equations for mesons and electromagnetic fields are solved self-consistently by expanding the Dirac spinors and the fields with harmonic oscillator bases up to $N_F = N_B = 14$ shells.

Table I compares the binding energies E of superheavy element $^{293}118$ and its α decay daughter nuclei calculated with effective forces TM1 [17], NL1 [18], NL3 [19], and NLSH [20]. The K-quantum number and the parity of the last filled neutron orbit are also shown. For comparison, the results of the phenomenological FRDM calculations are given in the last column [21].

The results of TM1 are nearly the same as those of FRDM for $^{265}104$, $^{269}106$, $^{273}108$, $^{277}110$, and $^{281}112$. They are within 1 MeV from each other. The difference between TM1 and FRDM results gets larger for $^{285}114$, $^{289}116$, and $^{293}118$, but is still smaller than 3 MeV. Though NL1, NL3, and NLSH give similar results as TM1, TM1 agrees most closely with FRDM.

One important difference between the RMF calculations with TM1 and FRDM is that the additional gain of the binding energy when one moves from $^{281}112$ to $^{285}114$ is much less in the RMF calculations. In other words, $Z = 114$ has a weaker meaning as a magic number in the RMF calculations. Though, strictly speaking, it may not be adequate, let us call this effect the change of the shell structure or the magic number property at $Z = 112$. As we shall see shortly, a similar effect appears in the Z dependence of the nuclear shape.

Table II shows the Q values of the ground-state–to–ground-state α decay sequence, $Q_{\alpha} = E(^{4}\mathrm{He}) + E(Z-2, N-2) - E(Z,N)$ (MeV), for RMF calculations with different forces and by FRDM. The Q values given by TM1 and FRDM are quite similar except for $^{285}114$, where the difference is 3.8 MeV. This large difference is caused by the change of the shell structure mentioned above.

Table III shows the corresponding deformation parameter β in the ground state. TM1 predicts a stable prolate deformation $\beta \sim 0.2$ for all the nuclei listed in the table, taking the minimum at $^{281}112$. NLSH gives similar results as TM1, though the minimum deformation is shifted to $^{289}116$ for NL3. The NL1 predicts a spherical shape for $^{293}118$, NL3 predicts a spherical shape for $^{289}116$ and $^{293}118$, while FRDM almost spherical shape for $^{281}112$, $^{285}114$, $^{289}116$, and $^{293}118$. The shift of the atomic number, where the deformation becomes minimum, from $Z = 114$ to 112 corresponds to what we already mentioned as evidence of the change of the shell structure concerning the binding energy.

Table IV compares the corresponding charge-radii R_c. In contrast to the large difference seen in the binding energy, the charge-radii R_c for different forces lie within 1% from each other.

III. PAIRING CORRELATION IN SUPERHEAVY ELEMENTS: DESCRIPTION BY RCHB

In this section we study the effects of pairing correlation in superheavy element $^{293}118$ and its α decay daughter nu-

TABLE II. The Q values of the ground-state–to–ground-state α decay for superheavy element $^{293}118$ and its α decay daughter nuclei. We used the experimental value 28.3 MeV for the binding energy of the α particle.

$^{A}Z_{N}$	TM1	NL1	NL3	NLSH	FRDM
$^{269}106_{163}$	8.3	7.2	8.7	1.3	7.8
$^{273}108_{165}$	8.3	9.6	8.1	7.9	9.4
$^{277}110_{167}$	10.6	10.6	10.0	10.1	10.7
$^{281}112_{169}$	10.0	9.0	9.6	9.7	10.1
$^{285}114_{171}$	13.2	6.3	10.9	14.3	9.4
$^{289}116_{173}$	11.4	11.4	11.3	11.4	11.3
$^{293}118_{175}$	11.8	8.1	10.6	13.4	12.2

TABLE III. The deformation β of the superheavy element $^{293}118$ and its α decay daughter nuclei calculated with effective interactions TM1, NL1, NL3, and NLSH. The prediction of FRDM is also given in the last column.

$^{A}Z_{N}$	TM1	NL1	NL3	NLSH	FRDM
$^{265}104_{161}$	0.2656	0.2687	0.2528	0.2513	0.220
$^{269}106_{163}$	0.2059	0.2576	0.2030	0.2073	0.222
$^{273}108_{165}$	0.2021	0.2438	0.2000	0.2068	0.221
$^{277}110_{167}$	0.1857	0.2279	0.1749	0.1914	0.173
$^{281}112_{169}$	0.1681	0.2072	0.1650	0.1741	0.089
$^{285}114_{171}$	0.2118	0.1593	0.1575	0.2316	-0.096
$^{289}116_{173}$	0.2373	0.1548	0.0653	0.2566	0.080
$^{293}118_{175}$	0.2340	0.0600	0.0601	0.2946	0.080

clei by using the self-consistent and fully microscopic RCHB theory [14] under the constraint of a spherical shape. With the pairing gap obtained in this way, a self-consistent and more complete RMF calculation including deformation will be carried out in the next section.

Before applying the RCHB theory to superheavy elements, we examine once again which effective force is most suitable to describe them by using lead isotopes as test cases.

The details of the calculations closely follow Refs. [14,15]. With the step size of 0.1 fm and using proper boundary conditions, the RCHB equations are solved in a spherical box of radius $R=20$ fm. As shown in Refs. [14,15] the results do not depend on the box size for $R \geqslant 20$ fm. A density-dependent force of zero range,

$$V(\boldsymbol{r}_1,\boldsymbol{r}_2)=\frac{V_0}{2}(1+P^{\sigma})\,\delta(\boldsymbol{r}_1-\boldsymbol{r}_2)\left[1-\rho\left(\frac{\boldsymbol{r}_1+\boldsymbol{r}_2}{2}\right)\Big/\,\rho_0\right], \tag{1}$$

is used for the pairing interaction as in Refs. [14,15]. Since we use a pairing force of zero range we have to limit the number of levels by a cutoff energy. For each spin-parity channel 15 radial wave functions are taken into account, which correspond roughly to a cutoff energy of 120 MeV for $R=20$ fm. For fixed cutoff energy and for fixed box radius R the strength V_0 of the pairing force for neutrons is determined so as to reproduce the pairing energy in ^{202}Pb given by the RCHB calculation using the finite range part of the Gogny D1S force [22]. The strength V_0 of the pairing force is then fixed for all the later calculations including superheavy elements. The same pairing force has been assumed for protons and neutrons. For ρ_0 we use the nuclear matter density 0.152 fm^{-3}. Our pairing interaction thus contains no free parameter (see Refs. [23,14,15] for details).

TABLE IV. Comparison of the charge-radii R_c of superheavy element $^{293}118$ and its α decay daughter nuclei calculated with different parameter sets.

$^{A}Z_{N}$	TM1	NL1	NL3	NLSH
$^{269}106_{163}$	6.146	6.153	6.122	6.104
$^{273}108_{165}$	6.174	6.176	6.150	6.134
$^{277}110_{167}$	6.197	6.203	6.178	6.158
$^{281}112_{169}$	6.226	6.228	6.200	6.188
$^{285}114_{171}$	6.282	6.248	6.227	6.250
$^{289}116_{173}$	6.332	6.272	6.243	6.303
$^{293}118_{175}$	6.360	6.276	6.261	6.355

The binding energies of six Pb isotopes calculated by RCHB in this way with four different effective forces are compared with experimental data in Table V. Although all the calculations reproduce well the experimental binding energies of the Pb isotopes, TM1 gives the best reproduction of the data. Therefore, we expect that the RMF calculations with TM1 and pairing correlation will give a good description of superheavy elements. The rms radii for neutrons R_N, protons R_P, matter R_M, and charge radii R_C calculated by the RMF with TM1 are given in the last four columns in Table V.

We have then calculated the binding energy E, matter and charge rms radii R_m and R_c, neutron and proton pairing gaps for superheavy elements in the RCHB with TM1 and NL3. The blocking effect for neutrons is taken into account in the same way as in Ref. [14], i.e., the blocking orbital for neutrons is the last filled neutron orbital. The results are shown in Table VI. The matter rms radius R_m is larger than the charge rms radius R_c for all nuclei due to the neutron excess. The proton pairing gap parameter is around 1 MeV, while the neutron pairing gap parameter is relatively small due to the blocking effect. The calculation for ^{86}Kr, ^{208}Pb, and $^{294}118$ are also given for reference to understand the fusion barrier to synthesize the element $^{294}118$.

TABLE V. Comparison of the binding energies E of Pb isotopes calculated in RCHB theory with 4 different parameter sets with experimental data. The last four columns are the root-mean-square neutron, proton, matter, and charge radii calculated with the TM1 parameter set.

A(Pb)	Expt. (MeV)	TM1	NL1	NL3	NLSH	R_N	R_P	R_M	R_C
202	1592.20	1592.91	1596.60	1592.69	1596.00	5.629	5.420	5.545	5.479
204	1607.52	1609.18	1611.35	1608.84	1611.35	5.656	5.429	5.566	5.487
206	1623.40	1623.78	1625.73	1624.58	1626.11	5.683	5.437	5.586	5.495
208	1636.45	1637.76	1639.72	1639.48	1639.99	5.713	5.447	5.609	5.505
210	1645.57	1646.92	1646.78	1647.06	1648.34	5.743	5.467	5.636	5.525
212	1654.52	1655.73	1653.57	1654.52	1656.43	5.772	5.486	5.663	5.544

TABLE VI. The binding energy E, matter and charge rms radii R_m and R_c, neutron and proton pairing gaps in RCHB with TM1 and NL3 for the superheavy element $^{293}118$ and its α decay daughter nuclei. The results for ^{86}Kr, ^{208}Pb, and $^{294}118$ are also given.

^AZ_N	TM1				NL3			
^AZ_N	E	R_m	R_c	Δ_n/Δ_p	E	R_m	R_c	Δ_n/Δ_p
$^{86}Kr_{50}$	750.2	4.221	4.182	-0.010/-1.304	748.6	4.211	4.171	-0.011/-1.268
$^{208}Pb_{126}$	1637.6	5.649	5.541	−0.000/−0.000	1639.5	5.631	5.517	−0.000/−0.000
$^{265}104_{161}$	1944.4	6.175	6.099	−0.622/−1.173	1940.0	6.164	6.088	−0.415/−0.724
$^{269}106_{163}$	1965.6	6.202	6.131	−0.421/−1.146	1961.9	6.189	6.118	−0.036/−0.577
$^{273}108_{165}$	1986.8	6.228	6.160	−0.283/−1.133	1983.0	6.214	6.144	−0.013/−0.734
$^{277}110_{167}$	2007.2	6.255	6.189	−0.380/−1.092	2003.2	6.240	6.172	−0.281/−0.771
$^{281}112_{169}$	2027.1	6.281	6.218	−0.338/−1.030	2023.3	6.266	6.200	−0.259/−0.740
$^{285}114_{171}$	2046.8	6.308	6.247	−0.030/−0.948	2043.3	6.293	6.228	−0.033/−0.680
$^{289}116_{173}$	2065.2	6.333	6.273	−0.013/−0.841	2062.0	6.318	6.253	−0.014/−0.595
$^{293}118_{175}$	2082.1	6.356	6.296	−0.315/−0.696	2079.0	6.341	6.276	−0.237/−0.466
$^{294}118_{176}$	2088.8	6.364	6.299	−0.442/−0.702	2085.8	6.349	6.279	−0.331/−0.466

In Figs. 1 and 2, the neutron and proton single-particle levels in the canonical basis in $^{292}118$ are given, respectively. In order to avoid the complexity due to the blocking effect, we give the single-particle levels in $^{292}118$ instead of $^{293}118$. The potential (the thick solid line) is the sum of the vector and scalar potentials. The Fermi surface for neutrons and protons is given in each figure by the dashed line. The Fermi level for neutrons in $^{293}118$ is at $\lambda=-6.304$ MeV, while that for protons at $\lambda=-1.916$ MeV. Although the Fermi level for protons is very close to the continuum, the wave functions of all the protons are well localized in a small region because of the Coulomb barrier.

Figure 1 indicates that, after the subclosed shell at $N=164$, the next closed or subclosed shells occur at $N=198$ and $N=210$, while Fig. 2 indicates that the closed or subclosed shells for protons occur at $Z=106$, $Z=114$, and $Z=120$. The magicity of a particular atomic or the neutron number depends, however, on the N or Z numbers, and also on deformation or vise versa. Figures 3 and 4 show the change of the single-particle neutron and proton levels near the Fermi surface along the α-decay chain from $^{293}118$. Similarly to Figs. 1 and 2, we give the single-particle levels for the neighboring even-even nuclei in order to avoid the irregularity due to the blocking effect. Adding an α particle always raises the proton single-particle levels and lowers the neutron single-particle levels. There are distinct gaps of about 2 MeV at $N=164$ and 172 and of about 3 MeV at $N=198$ for neutrons.

IV. THE DESCRIPTION OF SUPERHEAVY ELEMENTS BY RMF+BCS

Using the pairing gap for protons and neutrons from spherical RCHB calculations in Sec. III, we now perform the RMF + BCS calculations by including both deformation and pairing correlation. The blocking effect for neutrons is taken into account. The results for the binding energy E, the α-particle energy for the ground-state–to–ground-state decay Q_{gg}, matter and charge radii, and the neutron, proton, and matter deformation parameters are given in Tables VII and VIII for the TM1 and NL3 forces, respectively. The calculated binding energies for ^{86}Kr, ^{208}Pb, and $^{294}118$ are also given. Each binding energy increases by 0.3–2 MeV with the pairing correlation, and can noticeably alter the atomic number dependence of Q_α. The K-quantum number and the parity of the last neutron does not change from those in the calculations without pairing correlation for the ground state and are the same as those given in Table I.

One important aspect of the α decay of odd mass nuclei is a selection rule imposed by quantum numbers, e.g., the ground state (g.s.) to g.s. α decay will sometimes be structurally forbidden since the g.s. properties of the parent and daughter nuclei differ dramatically as indicated by the K-quantum number and the parity in Table I.

There are many possibilities to block levels. As examples, Table IX shows the binding energies E and the corresponding Q_α values calculated in the RMF theory with TM1 and NL3 forces when the α decay chain follows the K-quantum

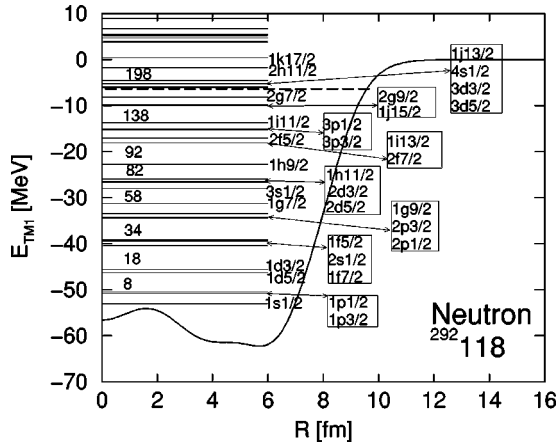

FIG. 1. The single-particle levels in the canonical basis for neutrons in $^{292}118$ calculated by RCHB with TM1. The neutron potential $V_V(r)+V_S(r)$ is represented by the solid line and the Fermi level by a dashed line.

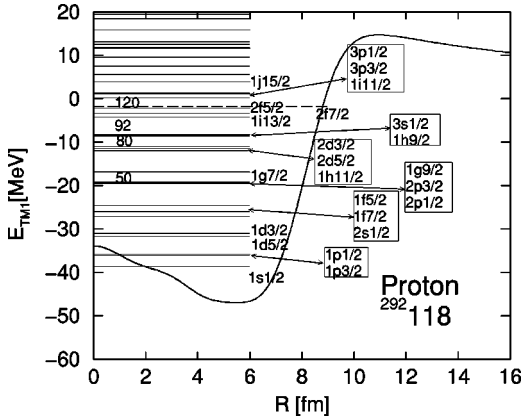

FIG. 2. The same as Fig. 1, but for protons.

number either $\Omega^{\pi}=1/2^{+}$ or $3/2^{+}$. As mentioned before, the calculations have been performed by using the pairing gap from RCHB for protons and neutrons, while the blocking levels for neutron are the $1/2^{+}$ and $3/2^{+}$ levels, respectively. The blocking in the levels $3/2^{+}$ and $1/2^{+}$ is chosen, because $3/2^{+}$ is the ground state for all interactions and $1/2^{+}$ is the first excited state for the TM1 force in $^{293}118$. For TM1 and NL3, the binding energies E and the Q values for the α decay given by both blocking $\Omega^{\pi}=1/2^{+}$ and $3/2^{+}$ may have a difference of 2 MeV in some cases.

In Fig. 5, the α-decay energy Q_{α} calculated by the RMF with TM1 and NL3 is shown as a function of the atomic number along the decay chain from $^{293}118$. The results for TM1 (NL3) are represented by filled (open) symbols and connected by solid (dashed) lines. The diamonds are the ground-state–to–ground-state Q values Q_{gg}, while the triangles up or down are those when the $1/2^{+}$ or $3/2^{+}$ neutron level is blocked. The observed data taken from Fig. 4 in [4], the prediction of FRDM [21], and the calculation of RMF with NLZ2 parameter sets for the ground states [24] are also shown.

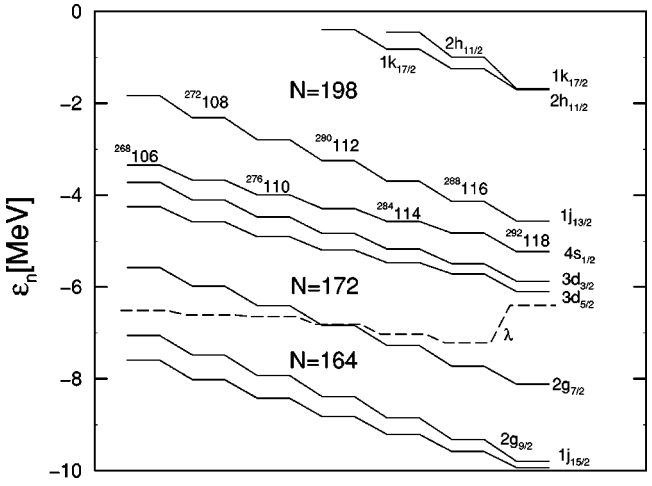

FIG. 3. The single-particle levels for neutrons near the Fermi surface calculated in the RCHB with TM1. They are shown for the neighboring even-even nuclei to the superheavy elements in the α-decay chain from $^{293}118$.

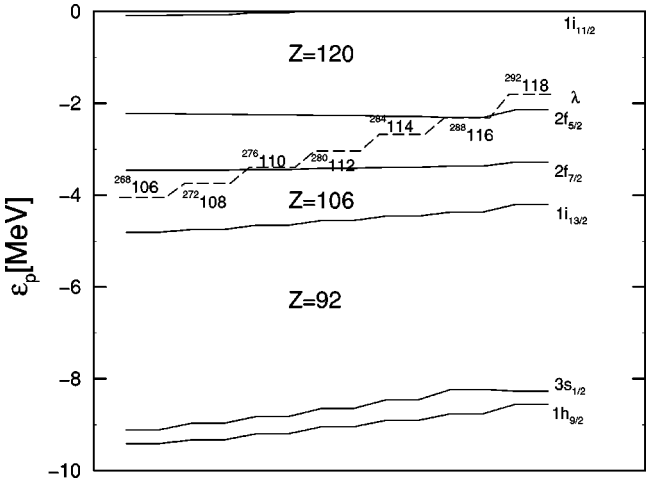

FIG. 4. The same as Fig. 3, but for protons.

The comparison between the triangles and diamonds clearly shows a noticeable discrepancy of the atomic number dependence and of the magnitude of the Q values for the ground-state–to–ground-state α decay and for the decay along a fixed K-quantum number. This is common in the RMF calculations with TM1 and NL3 forces. One also notices a clear difference of the Q values for the ground-state–to–ground-state α decay Q_{gg} between the RMF calculations with TM1 and FRDM, despite that the TM1 force was chosen among different RMF parameter sets because of its best global agreement with the prediction of the FRDM. A sharp difference is that Q_{gg} takes a local minimum at $Z=114$ in FRDM, while it takes a peak there in the RMF calculations. This reflects the shift of the magicity in two approaches which we discussed before. It is interesting to notice that the experimental data also shows a slight peak at $Z=114$. However, it will be premature to compare theoretical calculations with the data. Experimentally, it is not clear at all whether the decay proceeds along the ground state. Furthermore, the decay sequence can move to other places in the nuclear

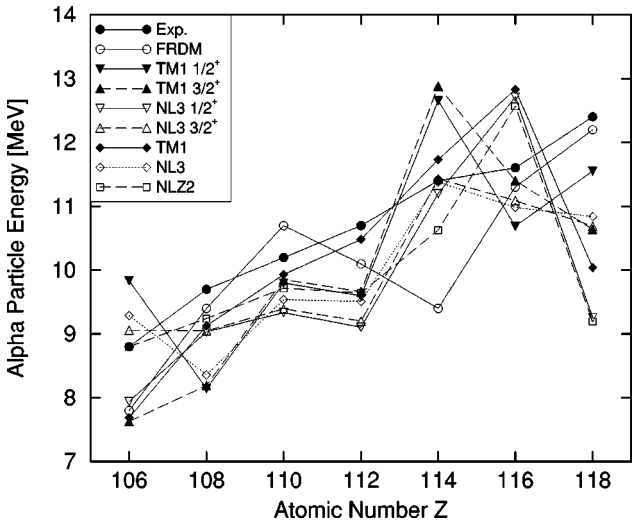

FIG. 5. Comparison of the theoretical α-particle energies Q_{α} with the observed data.

TABLE VII. The binding energy E, α-decay Q value Q_{gg}, matter and charge radii, and neutron, proton, and matter deformation parameters calculated in the RMF+BCS theory with TM1.

$^{A}Z_{N}$	E	Q_α	R_m	R_c	β_n	β_p	β
$^{86}Kr_{50}$	751.0		4.222	4.189	0.003	0.005	0.004
$^{208}Pb_{126}$	1636.8		5.650	5.544	0.000	0.000	0.000
$^{265}104_{161}$	1951.067		6.207	6.116	0.213	0.210	0.212
$^{269}106_{163}$	1971.674	7.69	6.233	6.148	0.209	0.208	0.208
$^{273}108_{165}$	1990.846	9.13	6.255	6.174	0.194	0.194	0.194
$^{277}110_{167}$	2009.211	9.93	6.278	6.202	0.178	0.178	0.178
$^{281}112_{169}$	2027.032	10.48	6.303	6.228	0.165	0.166	0.165
$^{285}114_{171}$	2043.601	11.73	6.324	6.252	0.149	0.152	0.150
$^{289}116_{173}$	2059.075	12.83	6.345	6.274	0.132	0.135	0.133
$^{293}118_{175}$	2077.022	10.04	6.354	6.289	0.062	0.058	0.060
$^{294}118_{176}$	2081.3		6.429	6.365	0.224	0.229	0.226

chart, because none of the observed α matches with known decay.

V. SUMMARY

We made a systematic study of the structure of superheavy elements recently claimed to have been discovered at Berkeley Lab's 88-Inch Cyclotron by the reaction $^{86}Kr + ^{208}Pb$ at 449 MeV in the framework of the relativistic mean field (RMF) approach. We have shown that usually used various RMF forces, which provide a fair description of normal stable nuclei, give different predictions for superheavy elements. Among them TM1 is found to be the best candidate to describe superheavy elements.

We have shown that the binding energy obtained from TM1 agrees with that of FRDM within a difference of 2 MeV. The same conclusion that TM1 is a good interaction has been drawn from the calculations of the binding energy of Pb isotopes using the relativistic continuum Hartree-Bogoliubov (RCHB) theory. We then performed RMF calculations of superheavy elements which include both the pairing correlation and deformation by using the pairing gaps obtained from RCHB for protons, and using the filling approximation for neutrons to simplify the blocking effect.

Our calculations suggest that the superheavy elements

TABLE VIII. The same as Table VII, but with NL3.

$^{A}Z_{N}$	E	Q_α	R_m	R_c	β_n	β_p	β
$^{86}Kr_{50}$	743.899		4.276	4.234	0.280	0.283	0.281
$^{208}Pb_{126}$	1639.48		5.631	5.517	0.000	0.000	0.000
$^{265}104_{161}$	1951.983		6.199	6.103	0.254	0.259	0.256
$^{269}106_{163}$	1970.990	9.29	6.214	6.128	0.215	0.218	0.216
$^{273}108_{165}$	1990.928	8.36	6.234	6.150	0.195	0.197	0.196
$^{277}110_{167}$	2009.688	9.54	6.256	6.176	0.175	0.176	0.175
$^{281}112_{169}$	2028.479	9.51	6.277	6.200	0.154	0.157	0.156
$^{285}114_{171}$	2045.400	11.38	6.287	6.220	0.057	0.062	0.058
$^{289}116_{173}$	2062.713	10.98	6.309	6.242	0.051	0.053	0.052
$^{293}118_{175}$	2080.174	10.84	6.330	6.262	0.058	0.053	0.056
$^{294}118_{176}$	2085.92		6.340	6.266	0.063	0.059	0.062

$^{293}118$ and its α decay daughter nuclei have finite deformation, having minimum deformation at $Z=112$, and also that the element $^{293}118$ has a small proton separation energy. We also discussed the Q values of the α decay sequence for both ground-state–to–ground-state transitions and for the decay along a fixed K quantum number. One interesting observation is that the predicted Q value has a peak at $Z=114$ in contrast to a minimum suggested by FRDM. This is a consequence of the shift of the magic number from 114 to 112. Unfortunately, one cannot compare theoretical results with experimental data, because it is not clear whether the observed α correspond to ground-state–to–ground-state decays or transitions to excited states. Even the location of the sequence might move in the nuclear chart, because all the observed α's do not match with the known α. Theoretically, it is very challenging to perform reliable predictions of the decay scheme, the corresponding Q values, and the lifetime of the α decays from the superheavy elements, not only those suggested by the experiment at Berkeley, but also those for a well-accepted $Z=112$ [3] and those suggested by the experiments in Ref. [26].

After we completed our study, we noticed a paper by Cwiok *et al.* [25], which discusses the properties of the same sequence of superheavy elements and their α decay properties in nonrelativistic HFB calculations. It is interesting to notice that their nonrelativistic calculations predict quite different properties from what we obtained using the RMF ap-

TABLE IX. The binding energy E and the Q value for the α decay Q_α for the $\Omega^\pi = 1/2^+$ *or* $3/2^+$ level blocking in RMF with TM1 and NL3.

Nucleus	TM1				NL3			
$^{A}Z_{N}$	$E(1/2^+)$	Q_α	$E(3/2^+)$	Q_α	$E(1/2^+)$	Q_α	$E(3/2^+)$	Q_α
$^{265}104_{161}$	1951.043		1949.174		1950.531		1951.983	
$^{269}106_{163}$	1969.509	9.834	1969.841	7.633	1970.887	7.944	1971.223	9.060
$^{273}108_{165}$	1989.665	8.144	1989.948	8.193	1990.150	9.037	1990.473	9.050
$^{277}110_{167}$	2008.168	9.797	2008.395	9.853	2009.115	9.335	2009.381	9.392
$^{281}112_{169}$	2026.871	9.597	2027.031	9.664	2028.308	9.107	2028.479	9.202
$^{285}114_{171}$	2042.520	12.65	2042.454	12.88	2045.405	11.20	2045.353	11.43
$^{289}116_{173}$	2060.127	10.69	2059.358	11.40	2060.999	12.71	2062.561	11.09
$^{293}118_{175}$	2076.876	11.55	2077.022	10.64	2080.044	9.255	2080.174	10.69

proach. They predict systematically much smaller deformation for all nuclei and also claim that the deformation monotonically decreases towards $Z=118$. Reflecting the different prediction concerning the deformation in our calculations and in Ref. [25], the K-quantum numbers of the last neutron are very different in the two studies. This difference will lead to quite different predictions for the α decay properties. Further studies are certainly needed to understand well the properties and the decay scheme of superheavy elements.

ACKNOWLEDGMENTS

J.M. thanks the Department of Physics, Tohouku University for its hospitality and acknowledges the financial support of Japan Society for the Promotion of Science for making his stay possible. This work was partially sponsored by the National Science Foundation in China under Projects No. 19847002 and No. 19935030, and by SRF for ROCS, SEM, China.

[1] S. Hofmann *et al.*, Z. Phys. A **350**, 277 (1995).
[2] S. Hofmann *et al.*, Z. Phys. A **350**, 281 (1995).
[3] S. Hofmann *et al.* Z. Phys. A **354**, 229 (1996).
[4] V. Ninov *et al.*, Phys. Rev. Lett. **83**, 1104 (1999).
[5] A. Iwamoto, P. Moller, J. Rayford Nix, and H. Sagawa, Nucl. Phys. **A596**, 329 (1996).
[6] C.L. Wu, M. Guidry, and D.H. Feng, Phys. Lett. B **387**, 449 (1996).
[7] G.A. Lalazissis, M.M. Sharma, P. Ring, and Y.K. Gambhir, Nucl. Phys. **A608**, 202 (1996).
[8] S. Cwiok, J. Dobaczewski, P.-H. Heenen, P. Magierski, and W. Nazarewicz, Nucl. Phys. **A611**, 211 (1996).
[9] K. Rutz, M. Bender, T. Buervenich, T. Schilling, P.-G. Reinhard, J. A. Maruhn, W. Greiner, Phys. Rev. C **56**, 238 (1997).
[10] G.G. Adamian, N.V. Antonenko, W. Scheid, and V.V. Volkov, Nucl. Phys. **A633**, 409 (1998).
[11] M. Bender, K. Rutz, P.-G. Reinhard, J.A. Maruhn, and W. Greiner, Phys. Rev. C **58**, 2126 (1998).
[12] R. Smolanczuk, Phys. Rev. C **60**, 1301 (1999).
[13] R. Smolanczuk, Phys. Rev. C **56**, 812 (1997).
[14] J. Meng, Nucl. Phys. **A635**, 3 (1998).
[15] J. Meng and P. Ring, Phys. Rev. Lett. **77**, 3963 (1996); **80**, 460 (1998).
[16] Y.K. Gambhir, P. Ring, and A. Thimet, Ann. Phys. (N.Y.) **194**, 132 (1990).
[17] Y. Sugahara and H. Toki, Nucl. Phys. **A579**, 558 (1994).
[18] P.G. Reinhard, M. Rufa, J. Maruhn, W. Greiner, and J. Friedrich, Z. Phys. A **323**, 13 (1986).
[19] G.A. Lalazissis, J. König, and P. Ring, Phys. Rev. C **55**, 540 (1997).
[20] M.M. Sharma, M.A. Nagarajan, and P. Ring, Phys. Lett. B **B312**, 377 (1993).
[21] P. Moller *et al.*, At. Data Nucl. Data Tables **59**, 185 (1995).
[22] J.F. Berger *et al.* Nucl. Phys. **A428**, 32c (1984).
[23] J. Meng, Phys. Rev. C **57**, 1229 (1998).
[24] M. Bender, Phys. Rev. C **61**, 031302 (2000).
[25] S. Cwiok, W. Nazarewicz, and P.H. Heenen, Phys. Rev. Lett. **83**, 1108 (1999).
[26] Yu. Ts. Oganessian *et al.*, Phys. Rev. Lett. **83**, 3154 (1999).